ELSEVIER

International Journal of Minerals, Metallurgy and Materials
Volume 16, Number 1, February 2009, Page 84

Materials

Corrosion behavior of aluminum alloys in Na_2SO_4 solution using the scanning electrochemical microscopy technique

He-rong Zhou[1,2], *Xiao-gang Li*[1,2], *Chao-fang Dong*[1], *Kui Xiao*[1], *and Tai Li*[1]

1) School of Materials Science and Engineering, University of Science and Technology Beijing, Beijing 100083, China
2) Beijing Key Laboratory for Corrosion, Erosion and Surface Technology, Beijing 100083, China
(Received 2008-02-15)

Abstract: The corrosion behavior of aluminum alloys 1060 and 2A12 in a 10 mM Na_2SO_4+5 mM KI solution was investigated by scanning electrochemical microscopy (SECM) and scanning electron microscopy (SEM). The potential topography and corrosion morphology results show that the potential of the sample surface over the same area changes with the increase of immersion time. The corrosion area becomes large, and the potential becomes more negative. The corrosion potential of the 2A12 alloy surface is lower than that of 1060 aluminum, and 2A12 alloy becomes easily corrosive. This is the reason that preferential dissolution in the boundary region of some intermetallic particles (IMPs) occurs and different dissolution behaviors are associated with different types of IMPs because of different potentials.

Key words: aluminum alloys; corrosion behavior; intermetallic particles; scanning electrochemical microscopy (SECM)

[*This study was financially supported by the National Natural Science Foundation of China (No.50499331) and the National Science and Technology Basic Conditional Platform (No.2005DTA10400).*]

1. Introduction

In aluminum alloys, Si, Zn, Fe, Mn, Cu, and Mg are introduced at various levels mainly to improve their mechanical strength. Various kinds of intermetallic precipitates (IMPs) might form in the alloys, and their influence on corrosion processes has to be studied in detail to understand the mechanism and, hence, to control the corrosion of Al alloys [1]. Because of the complexity of the microstructure of multi-component aluminum (Al) alloys, the mechanism of localized corrosion of Al alloys is still not completely understood, especially regarding the influence of various kinds of intermetallic precipitates on the alloys. Further studies are needed on the formation of pits at intermetallic compounds and deterministic factors in pit initiation, *e.g.*, second phase particles and the conditions of pit formation [2]. The local techniques (for instance, scanning electrochemical microscopy (SECM), atomic force microscopy (AFM), and scanning Kelvin probe force microscopy (SKPFM)) have also been shown capable of providing useful information [3-5].

SECM, able to map the variations in local electrochemical activity, has been used to study pitting corrosion around MnS inclusions in stainless steels in NaCl solution [6-7]. It was also utilized to spatially resolve the heterogeneous cathodic activity at AA2024 surfaces by using Pt microelectrode and redox mediator [8]. The SECM images showed locally high redox reactivity that was attributed to intermetallic particles. In some reports, the SECM mapping was quite useful for corrosion behavior study.

The results of the SECM probing of local corrosion of aluminum alloys in sodium sulfate solutions were presented in this article, including the SEM observation of localized corrosion in the boundary region, and it is explained by the corrosion theory of IMPs.

2. Experimental

The experimental materials used are commercial 1060 aluminum and 2A12 aluminum alloy (2A12 alloy). The chemical composition (wt%) of the 1060 aluminum sample is Fe 0.36, Si 0.061, Mn 0.02, Mg

Corresponding author: He-rong Zhou, **E-mail:** zhouhr_9@sina.como
Also available online at www.sciencedirect.com

0.02, Zn 0.005, and balanced Al. The chemical composition (wt%) of 2A12 alloy is Fe 0.35, Si 0.13, Mn 0.53, Mg 1.58, Zn 0.10, Cu 4.68, Ti 0.023, and balanced Al. The samples were mounted in a low viscosity epoxy leaving 1 cm^2 exposed surface area. The sample surface was ground with SiC paper up to 4000 grit, and then, polished with 1.5 and 0.5 mm diamond paste, using 99.5vol% ethanol. The sample was fixed in an electrochemical cell made of Teflon, a saturated Ag/AgCl was used as the reference electrode, and a Pt foil surrounding the sample as the counter electrode (Fig. 1).

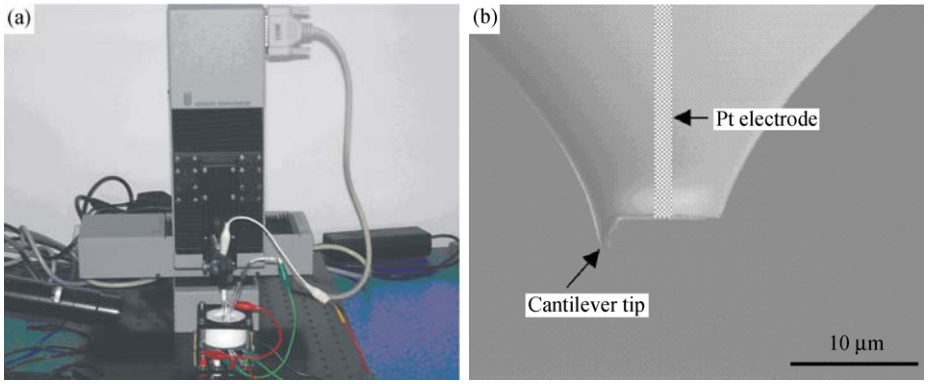

Fig. 1. SECM instrument and electrochemical cell (a) and mode probe for SECM measurement (b).

Reagent Na_2SO_4, KI, and distilled water were used to make up the solution (pH 5). The concentration of Na_2SO_4 was 10 mM, and 5 mM KI was added as the redox mediator for SECM mapping because of the local corrosion process [4].

SECM experiments were carried out on M370 electrochemical workstation. The instrument defines three axes of translation for the probe tip. The *x*-*y* plane is defined as the plane of the aluminum alloy substrate electrode, and the *z* axis is defined as the axis normal to this plane. The surface morphology of the samples after corrosion was observed using SEM.

3. Results and discussion

3.1. Microstructure

Fig. 2 illustrates the SEM morphologies of aluminum alloys. The microstructure of 1060 aluminum consists of primary α-Al and Fe_3Al intermetallics (Fig. 2(a), dot A, *etc*.). Its amount of Fe_3Al intermetallic precipitates is small because of the Fe content. The microstructure of 2A12 alloy (T4) is composed of primary α-Al, θ phase (Al_2Cu), Al_2CuMg, and $(Al,Cu)_6(Fe,Cu)$ (Fig. 2(b), dots B, C and so forth) intermetallics inside grains [8-9]. The number and type of the intermetallics in 2A12 alloy are more than those in 1060 aluminum, and alike, the bulk of the intermetallics in 2A12 alloy is large. The intermetallics containing Cu and Fe are cathodic relative to the matrix and promote the dissolution of the matrix, whereas the intermetallics including Mg are anodic relative to the matrix and dissolve preferentially [10].

3.2. Potential topography

Under free immersion, the corrosion behavior is observed on the surface of the aluminum alloys within a reasonable experimental time. Fig. 3 shows the *in-situ* SECM observations of the localized corrosion of 1060 aluminum in a 10 mM Na_2SO_4+5 mM KI solution. The surface potential of 1060 aluminum is variable over the same area during the ongoing corrosion process. Fig. 3(a) reveals the potential image after 2-h immersion. The area of the potential between –0.14 and –0.15 V is about 80% of the testing area, nearly 18% between –0.15 and –0.16 V, and about 2% between –0.13 and –0.14 V. With the increase of immersion time, the corrosion area becomes larger, and the potential of the sample surface becomes more negative in Figs. 3(b)-3(d). The potential in Fig. 3(b) is between –0.15 and –0.16 V in the region of about 60% of the testing area, probably 40% of that between –0.13 and –0.15 V after 16 h-immersion. After 48-h corrosion, the area of the potential between –0.15 and –0.16 V is almost 50%, and about 50% between –0.17 and –0.18 V. This proves that the corrosion of the 1060 aluminum sample becomes very severe at the time of 48 h.

The result of continuous potential probing of 2A12 alloy in a 10 mM Na_2SO_4+5 mM KI solution is shown in Fig. 4. It shows the same results as Fig. 3. The surface area of the potential between –0.16 and –0.20 V is almost 98% of the testing area after 2-h immersion (Fig. 4(a)). With the increase of immersion time, the potential of the sample surface quickly becomes more negative. The area of the potential between –0.20 and –0.24 V is nearly 95% of the testing area, and about 4% between –0.24 and –0.28 V after 8-h immersion (Fig. 4(b)). After 48-h corrosion, the area of the potential between –0.20 and –0.24 V is almost 50%,

about 40% between –0.24 and –0.28 V, and probably 10% between –0.32 and –0.36 V (Fig. 4(d)). This reveals that the potential of the 2A12 alloy surface is more negative than that of 1060 aluminum, and 2A12 alloy becomes easily corrosive.

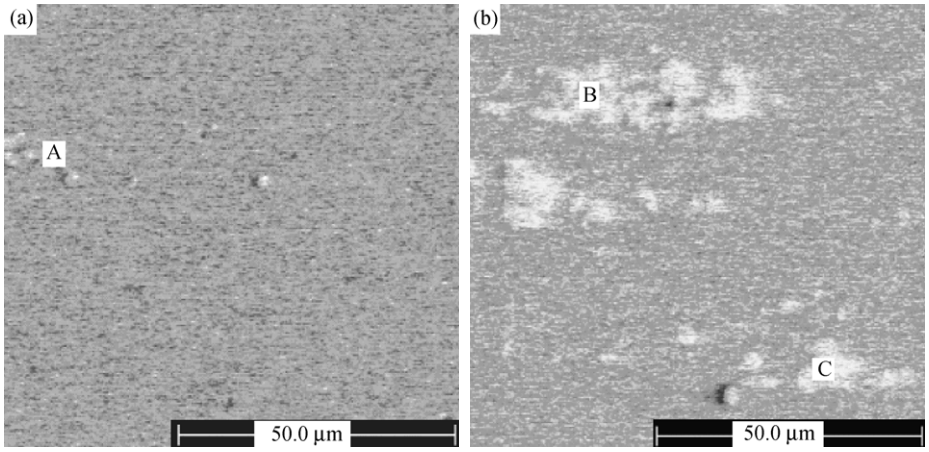

Fig. 2. Microstructures of 1060 aluminum (a) and 2A12 aluminum alloy (b).

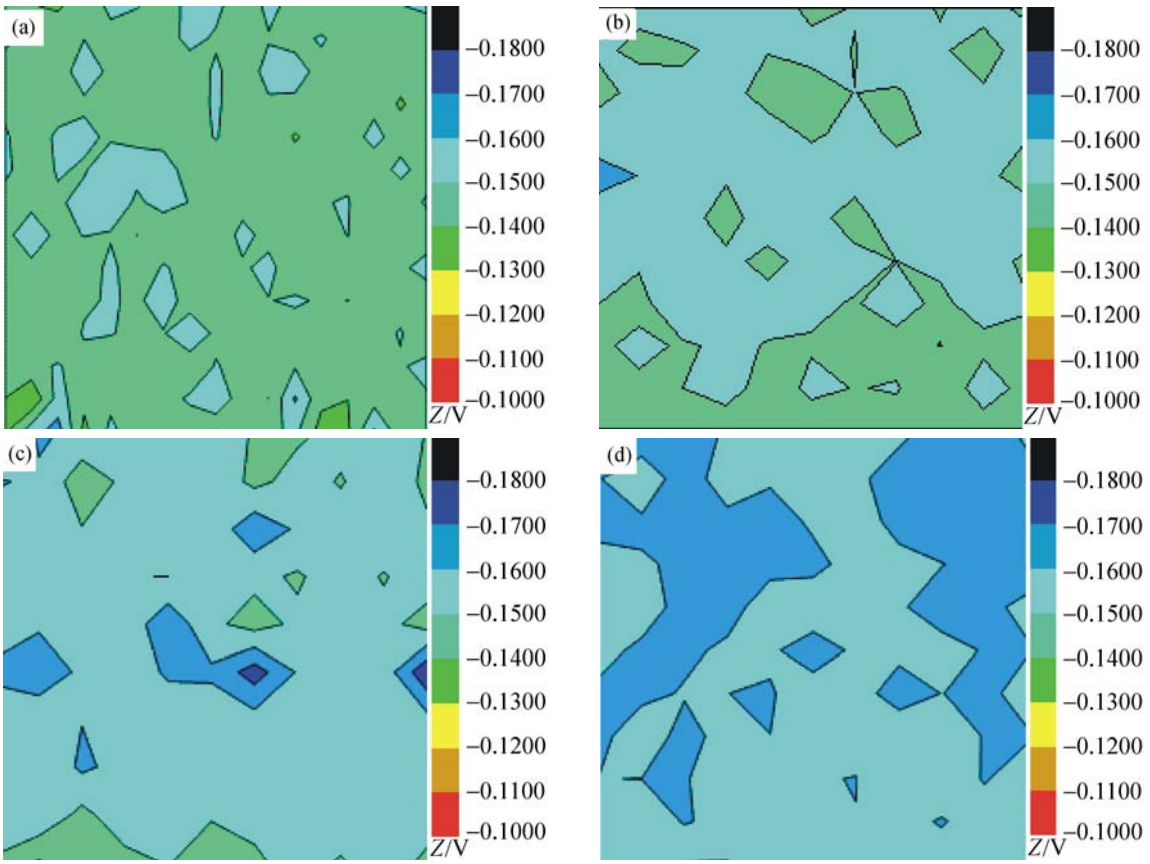

Fig. 3. Potential images of 1060 aluminum in a 10 mM Na_2SO_4+5 mM KI solution: (a) 2 h; (b) 16 h; (c) 23 h; (d) 48 h (scanning area: 400 μm×400 μm).

3.3. SEM morphology

SEM morphologies of 1060 aluminum in a 10 mM Na_2SO_4+5 mM KI solution after 48-h corrosion are shown in Fig. 5, and the corrosion morphologies of 2A12 alloy in Fig. 6. From the figures, the pitting occurs on the surface of aluminum alloys firstly, *i.e.*, localized dissolution. Because of low solution concentrations, corrosion is very slight for the two kinds of aluminum alloys. The number of the pits for 2A12 alloy is more than that of 1060 aluminum. The corrosion area becomes large. So the corrosion of 2A12 alloy is severer than that of 1060 aluminum. This is consistent with the above-mentioned potential results.

From the round-shaped corrosion morphologies (Figs. 5(a) and 6(a)), corrosion occurs inside the ring. Figs. 5(b) and 6(b) show the corrosion morphologies within the ring. Fig. 5(b) shows the dissolution products deposited on the surface of 1060 aluminum (Fig.

5(b), dots B and C). However, there are some pits and trenches on the surface of 2A12 alloy, a few products deposit on the surface. The crystal particle and boundary morphologies are clear. Localized dissolution occurs around a particle, pits, or the particle/matrix boundary region (Fig. 6(b), dots D, E, *etc*.).

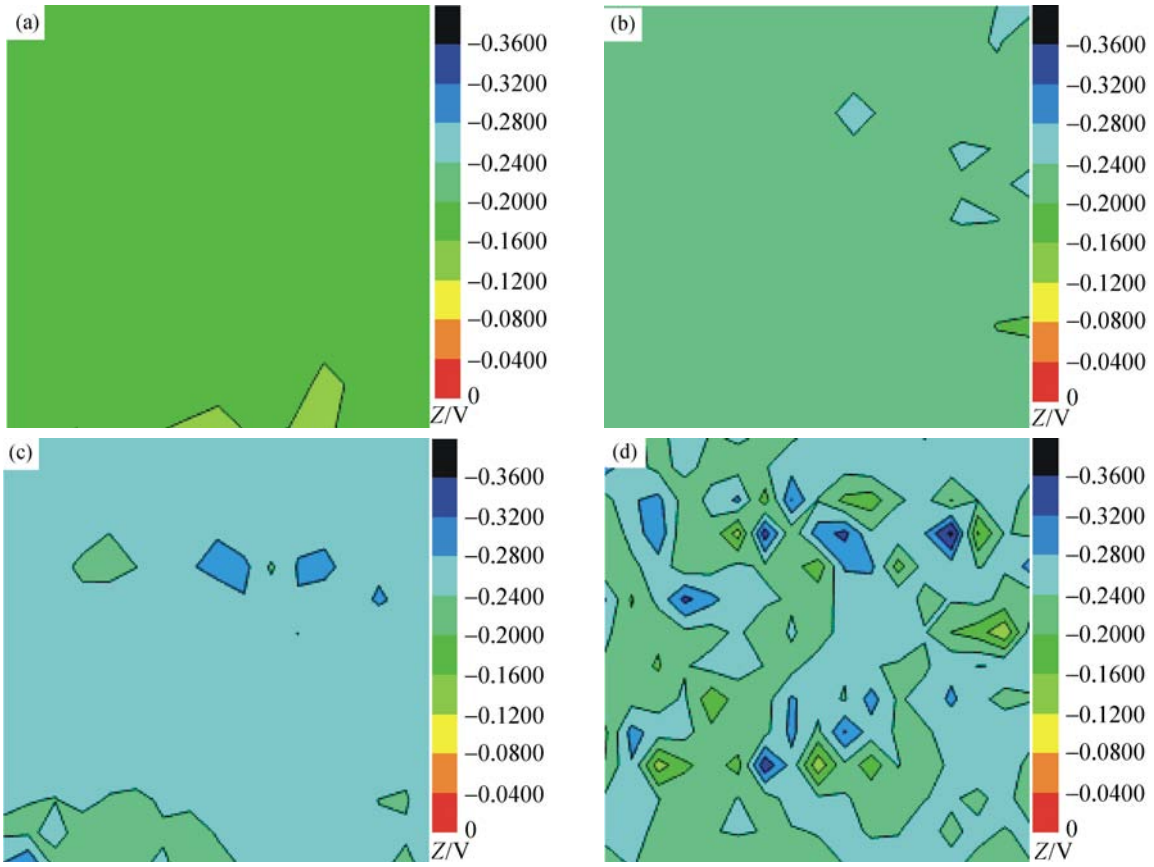

Fig. 4. Potential images of 2A12 alloy in a 10 mM Na_2SO_4+5 mM KI solution: (a) 2 h; (b) 8 h; (c) 28 h; (d) 48 h (scanning area: 400 μm×400 μm).

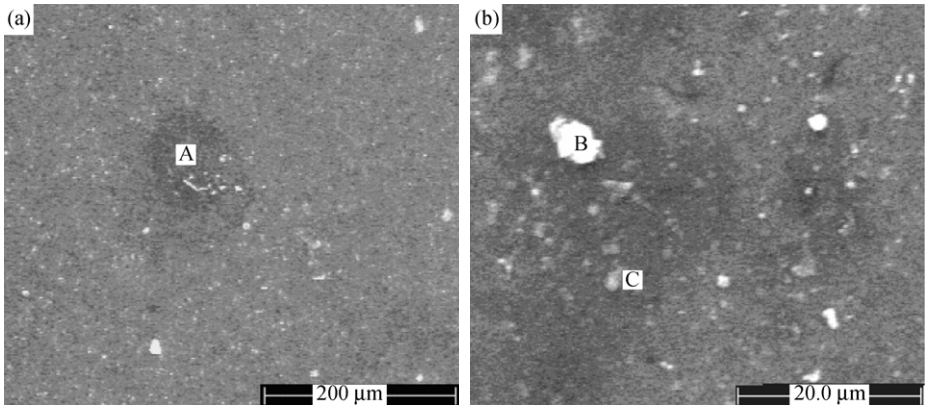

Fig. 5. SEM morphologies of pure aluminum 1060 in a 10 mM Na_2SO_4+5 mM KI solution after 48-h immersion.

3.4. Discussion

After the sample was immersed in the 10 mM Na_2SO_4 + 5 mM KI solution, localized corrosion (namely, localized dissolution) occurred in a particle, matrix, or the particle/matrix boundary region firstly, especially intermetallics inside grains [1]. During the ongoing corrosion process of aluminum alloys, different local dissolution behaviors were observed under SEM and SECM, which could be attributed to different types of IMPs. The intermetallics containing Cu and Fe promote the dissolution of the matrix, mainly the aluminum dissolved preferentially. The intermetallics rich in Mg are anodic relative to the matrix, dissolve preferentially and desquamate from the surface of the sample. The pit is formed on the surface lastly (Fig. 6(b), dot E) [11]. Perhaps, there are other corrosion spots, *e.g.*, defect, impurity, and so forth. So, the localized dissolution area is augmented and the trench comes into being in the boundary region finally (Figs. 6(b), dot D).

The potential of the sample surface appears to change and becomes low because of the dissolution. The potential of the local dissolution region becomes lower and the corrosion area becomes larger with the increase of immersion time. Local regions are anodic with respect to the matrix and dissolve firstly because of the low potential (as IMPs). At last, the pitting occurs and the pitting area increases (Fig. 6(b), dots A, B, C, and so on.) [3].

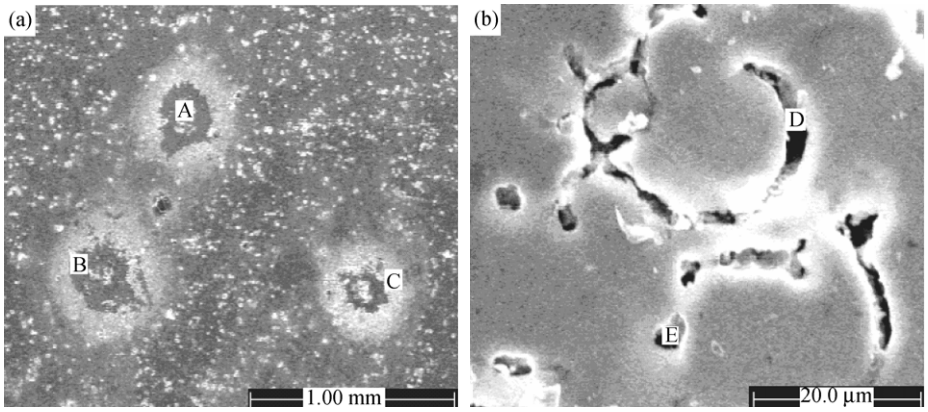

Fig. 6. SEM morphologies of 2A12 alloy in a 10 mM Na_2SO_4+5 mM KI solution after 48-h immersion.

There are some kinds of intermetallics for 2A12 alloy, such as Al_2Cu, Al_2CuMg, and $(Al, Cu)_6(Fe, Cu)$. Otherwise, 2A12 alloy contains more alloy elements and defects than 1060 aluminum. So there are possibly more anodic and cathodic sites for 2A12 alloy in the course of dissolution. And the potential of 2A12 alloy is more negative than that of 1060 aluminum. Therefore, 2A12 alloy becomes easily corrosive.

4. Conclusion

SECM and SEM are useful for corrosion probing of local dissolution for aluminum alloys. Different local dissolution behaviors in the particle/matrix boundary regions were observed under SEM, which can be attributed to different types of IMPs. Moreover, by using the SECM system, simultaneous probing of electrochemically active sites and topographic changes over the same area was accomplished during the ongoing corrosion process. The potential of the sample surface appears to change because of the local dissolution. The corrosion area becomes larger and the potential becomes more negative with the increase of immersion time. Moreover, the surface potential of 2A12 alloy is lower than that of 1060 aluminum, and 2A12 alloy becomes easily corrosive.

Acknowledgement

We thank Guo-zhe Meng in Harbin Engineering University for providing the M370 electrochemical workstation facilities.

References

[1] A. Davoodi, J. Pana, C. Leygraf, *et al*., Probing of local dissolution of Al-alloys in chloride solutions by AFM and SECM. *Appl. Surf. Sci.*, 252(2006), p.5499.

[2] Z.S. Smialowska, Pitting corrosion of aluminum, *Corros. Sci.*, 41(1999), p.1743.

[3] J.H.W. de Wit, Local potential measurements with the SKPFM on aluminium alloys, *Electrochim. Acta*, 49(2004), p.2841.

[4] A. Davoodi, J. Pan, C. Leygraf, and S. Norgren, *In situ* investigation of localized corrosion of aluminum alloys in chloride solution using integrated EC-AFM/SECM techniques, *Electrochem. Solid State Lett.*, 8(2005), No.6, p.B21.

[5] Y.H. Shao and M.V. Mirkin, Probing ion transfer at the liquid/liquid interface by scanning electrochemical microscopy, *J. Phys. Chem. B*, 102(1998), p.9915.

[6] C.H. Paik, H.S. White, and R.C. Alkire, Scanning electrochemical microscopy detection of dissolved sulfur species from inclusions in stainless steel, *J. Electrochem. Soc*., 147(2000), p.4120.

[7] E. Volker, C.G. Inchauspe, and E.J. Calvo, Scanning electrochemical microscopy measurement of ferrous ion fluxes during localized corrosion of steel, *Electrochem. Commun.*, 8(2006), p.179.

[8] J.C. Seegmiller and D.A. Buttry, A SECM study of heterogeneous redox activity at AA2024 surfaces, *J. Electrochem. Soc*., 150(2003), No.9, p.B413.

[9] R.G. Buchheit, M.A. Martinez, and L.P. Montes, Evidence for Cu ion formation by dissolution and dealloying the Al_2CuMg intermetallic compound in rotating ring—dish collection experiments, *J. Electrochem. Soc.*, 147(2000), p.119.

[10] R.G. Buchheit, R.P. Grant, P.F. Hlavaa, *et al*., Local dissolution phenomena associated with S phase (Al_2CuMg) particles in aluminum alloy 2024-T3, *J. Electrochem. Soc*., 144(1997), No.8, p.2621.

[11] F. Andreatta, M.M. Lohrengel, H. Terryn, *et al*., Electrochemical characterisation of aluminum AA7075-T6 and solution heat treated AA7075 using a micro-capillary cell, *Electrochim. Acta*, 48(2003), p.3239.